

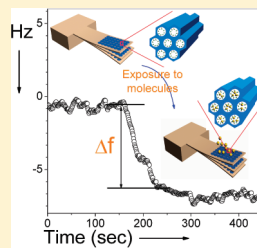
Functionalized Mesoporous Silica for Microgravimetric Sensing of Trace Chemical Vapors

Pengcheng Xu, Haitao Yu, and Xinxin Li*

State Key Lab of Transducer Technology, and Science and Technology on Microsystem Lab, Shanghai Institute of Microsystem and Information Technology, Chinese Academy of Sciences, Shanghai, People's Republic of China

 Supporting Information

ABSTRACT: Featuring a huge surface-to-volume ratio, synthesized SBA-15 mesoporous silica is functionalized by inner-channel-wall modification of sensing groups for highly specific chemical-vapor detection at trace level. With the developed sensing material loaded on resonant microcantilevers, the specifically adsorbed chemical-vapor molecules act as an added mass to shift the cantilever resonant frequency for gravimetric sensing signal readout. Two kinds of sensing materials for trinitrotoluene (TNT) and ammonia/amine are respectively prepared by inner-wall layer-by-layer grafting functionalization. By using hexafluoro-2-propanol-functionalized mesoporous silica (HFMS), experimental results show highly specific and rapid detection of TNT vapor, with a ppt-level detection limit; functionalized with a carboxyl (COOH) group, the mesoporous silica is loaded onto the cantilever resonating sensor that experimentally exhibits an ultrafine detection limit of tens of ppb to ammonia/amine gases.



On-the-spot rapid detection of trace chemical vapors with portable chemical sensors is highly demanded in environmental protection, industrial pollution control, biomedical systems, public safety guarantees, etc.^{1–4} In many such applications, the detection has to face formidable challenges due to the rather low concentration of target molecules,⁵ environment interference, and sensor miniaturization. Up to now, quite a lot of efforts have been made in exploring new sensing materials and transducers to build high-performance chemical microsensors.⁶ In the past decade, gravimetric-type chemical sensors have received intensive attention, such as chemical sensors that can indicate analyte molecules through direct readout of the frequency shift that is induced by a specific mass-adsorption. Compared to market-available gravimetric transducers such as the quartz crystal microbalance (QCM)⁷ and surface acoustic wave (SAW) devices,^{8–10} the resonant microcantilever¹¹ features the advantages of ultrafine resolvable minimum mass, reduced device size, on-chip integrated self-sensing elements such as piezoresistors, compatible integration with electronic circuits or other cantilevers into arrays, low-cost batch fabrication,^{12,13} etc. Thus, microcantilever sensors are promising for applications in microgravimetric detection of trace chemical vapors.

For microgravimetric bio/chemical sensing, the resonant microcantilever should be coated with a chemically sensitive layer for specific reaction with the target analyte molecules. For sensing relatively larger biomolecules or cells, the mass of a single layer adsorption is enough for gravimetric detection.^{14,15} Hence, specific self-assembled monolayers (SAMs) or a multilayer can be applied onto the cantilever surface for biomolecule-specific adsorption. However, to detect the relatively smaller molecules of some chemical vapors, the single-layer adsorbed mass is, more often than not, insufficient to be sensed. Therefore, new materials that possess higher specific surface area to provide more sensing sites should be considered for microgravimetric sensors. Recently developed advanced sensing materials include normal

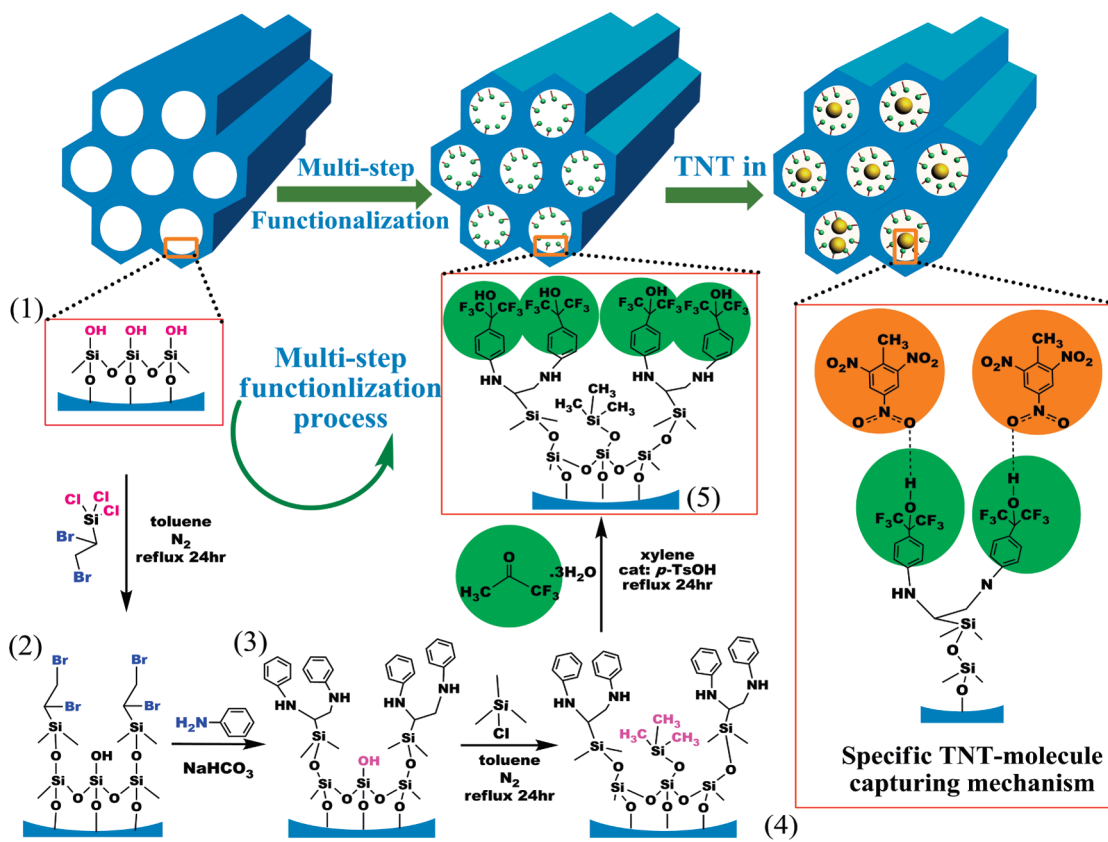
polymers,¹⁶ hyperbranched polymers,¹⁷ nanorods,^{18,19} and carbon nanotubes (CNTs).²⁰ Compared to the aforementioned materials, mesoporous materials undoubtedly feature much higher (up to 1500 m²/g) specific surface area.²¹ Nanoporous chemical sensing materials, including metal organic frameworks (MOFs), semiconductors, calixarenes, and mesoporous silica, have been used in various types of sensors such as stress-detection devices, chemiresistors, and electrochemical electrodes.^{22–30} Compared with the above-mentioned sensors, the resonant microcantilever is more suitable for using functionalized mesoporous silica to enhance the sensing performance. The huge specific surface area allows more molecules to be adsorbed, which leads to a higher mass-adding-induced frequency-shift sensing signal. To the best of our knowledge, functionalized mesoporous silica has been seldom used in gravimetric chemical sensors so far, possibly because the sensing group modification at the inner walls of the mesopores encounters the classic problem of “ship in a bottle”, i.e., it is difficult to assemble the building blocks into the nanopores as desired because of the nanoscopic confinement effect. Especially for detection of chemical molecules such as TNT, the specifically designed sensing groups are complicated and need multistep inner-channel layer-by-layer grafting processes.³¹ Furthermore, for adsorbing more target molecules, dense specific sensing groups should be functionalized on the high surface-area material. If the difficulty of inner-channel modification can be overcome, functionalized mesoporous materials are reasonably expected to be developed as high-performance sensing materials in microgravimetric sensors to significantly enhance the detection resolution of chemical vapors. On the other hand, the pore diameter (ranging from several to a

Received: January 7, 2011

Accepted: March 17, 2011

Published: April 04, 2011

Scheme 1. Schematic of HFIP Sensing Group Modification on the Inner Wall of SBA-15 Mesoporous Silica and the Specific Capturing Mechanism for TNT Molecules



couple of tens of nanometers that can be adjusted by the synthesis process) of mesoporous silica can be optimally constructed to capture the chemical molecules (whose sizes are on the same scale).

Since the pioneered work of Kresge et al.,³² mesoporous silica has been studies and widely applied in fields such as adsorption,³³ ion exchange,³⁴ drug delivery,³⁵ DNA translocation,³⁶ and catalysis.³⁷ So far, a series of mesoporous silicas with various mesostructures has been synthesized.^{32,38–42} SBA-15, a key member of the mesoporous silica family, was first explored in 1998.^{43,44} Compared with its counterparts, SBA-15 features controllable and adjustable pore size in the range of 4–30 nm and a thick pore wall (3–6 nm) that provides high stability.

In this study, SBA-15 mesoporous silica has been synthesized with highly specific and dense sensing groups modified onto the channel inner wall. Loaded with functionalized SBA-15 mesoporous silica sensing materials specific to trinitrotoluene (TNT) and ammonia/amine vapors, respectively, two high-performance integrated resonant microcantilever gravimetric sensors have been developed to detect each of these two kinds of trace chemical vapor. The micro/nano combined sensors have shown ultraresoluble detection capability to the ppt level of TNT and tens of ppb level of ammonia/amine vapors.

■ EXPERIMENTAL SECTION

HFMS Preparation. HFIP-functionalized mesoporous silica (HFMS) is prepared by following the steps of SBA-15 synthesis and then specific modification by using a multistep inner-channel

layer-by-layer grafting process. The technical details and sample-characterization results are provided in Table S1 and Figure S1 of Supporting Information.

COOH-Functionalized Mesoporous Silica (CMS) Preparation. A 1 mL amount of CES (carbomethoxysilanetriol, sodium salt, 25% in water, Gelest Inc.) is added into 30 mL of deionized water (DI water). Then concentrated HCl solution (12 M) is dropwise added to adjust the pH value to 4–5. A 0.2 g amount of SBA-15 mesoporous silica is added into the above-mentioned solution and stirred at 70 °C for 3 days. Next, the solution is filtered, and the solid is washed with DI water several times. Under vacuum, the solid COOH-functionalized mesoporous silica (CMS) product is dried at 60 °C.

Resonant Microcantilever Fabrication and Premodification. The cantilever is integrated with thermal–electric resonance excitation and piezoresistive signal readout elements. The resonant cantilever uses pulsed electric heating for thermal resonance excitation and a piezoresistive Wheatstone-bridge for signal readout. The length, width, and thickness of the cantilever are 200, 100, and 3 μm , respectively. Thus, the resonant frequency and effective mass can be calculated as about 101 kHz and 33 ng, respectively. With the resonant frequency and effective mass, the adsorbing mass sensitivity of the resonant microcantilever can be determined as 1.53 Hz/pg. The design and fabrication details of the resonant microcantilevers used in this research have been given elsewhere.¹⁷ In order to effectively suppress the interference signal from nonspecific adsorption of environmental moisture or organic molecules, the SiO_2 surface of the microcantilever is pretreated and passivated by self-assembling the molecules of

FAS-17 (heptadecafluorodecyltrimethoxysilane, Gelest Inc.) that feature ultralow surface energy. Such a superhydrophobic and oleophobic reagent can effectively mask the silanol groups at the SiO_2 cantilever surface.^{20,45} The premodification process is detailed in the Supporting Information.

VOC Sensor Preparation. A 0.01 g amount of as-prepared mesoporous sensing material is added into 1 mL DI water (under ultrasonic) to form a crude suspension. Then about 0.1 μL of suspension is loaded onto the cantilever top surface by using a commercial micromanipulator (Eppendorf, model: PatchMan NP2) with the aid of a microscope (Leica, model: DM4000). Then, the microcantilever is dried in an oven at 60 °C for about 2 h, at which time the VOC sensors are ready for detection experiments.

Sensing Experiment for VOCs. The sensing experiment is performed in a lab-made setup that contains three parts: frequency counter (Agilent, model S3131A), lab-made phase-lock-loop (PLL) interface circuit, and a series of testing chambers with the same constant volume (made of Pyrex glass). The technical details of vapor generation and concentration calibration are given in the Supporting Information.

■ RESULTS AND DISCUSSION

TNT-Sensing Material Design and Synthesis. Nitroaromatic compounds such as TNT can be selectively adsorbed by the sensing materials through hydrogen-bonding acidic groups.^{3,45} McGill et al. proposed a hydrogen-bonding model and developed advanced sensing groups for TNT detection.⁴⁶ According to their analytical and experimental results, benzene-ring-linked hexafluoro-2-propanol (HFIP) was determined as the specific TNT-sensing group. In this study, we graft the HFIP groups onto the inner surface of SBA-15 to construct HFIP-functionalized mesoporous silica (HFMS) as a new TNT-sensing material for cantilever-based gravimetric detection.

In general, there are two approaches to introduce the TNT-sensitive HFIP group onto the aromatic ring: (1) anhydrous hexafluoroacetone gas is used as a reagent to react with the benzene ring under an inert atmosphere, where anhydrous aluminum chloride is used as a catalyst;⁴⁷ (2) hexafluoro-2-propanol trihydrate liquid is used as a reagent to react with aniline derivatives in the presence of an acid.⁴⁸ In the former technique, preparation of highly purified anhydrous hexafluoroacetone gas is difficult, as the anhydrous hexafluoroacetone has a strong reactivity to trace moisture to yield a white-colored solid of hexafluoroacetone sesquihydrate, and this solid easily blocks the synthetic pipeline. In addition, anhydrous hexafluoroacetone gas is highly toxic, which increases the difficulty of preparation. In contrast, the latter method is relatively nontoxic and more easily performed in liquid; on the basis of these advantages, this method was adopted for our experiment.

Scheme 1 shows the schematic of the HFIP sensing group grafting process onto the inner channel walls of SBA-15 mesoporous silica and the mechanism of specifically capturing TNT molecules. With hexafluoro-2-propanol trihydrate as the raw material, ultradense functionalization of dual sensing groups per molecule chain is performed through layer-by-layer grafting. Before self-assembly, silanol ($\equiv\text{Si}-\text{OH}$) density at the inner-pore surface is enhanced by hydrating pretreatment.⁴⁹ Via reaction between $\equiv\text{Si}-\text{OH}$ and $\equiv\text{Si}-\text{Cl}$, the first monolayer is constructed where one molecule chain bears two Br groups. With aniline added, the two Br groups are substituted by two

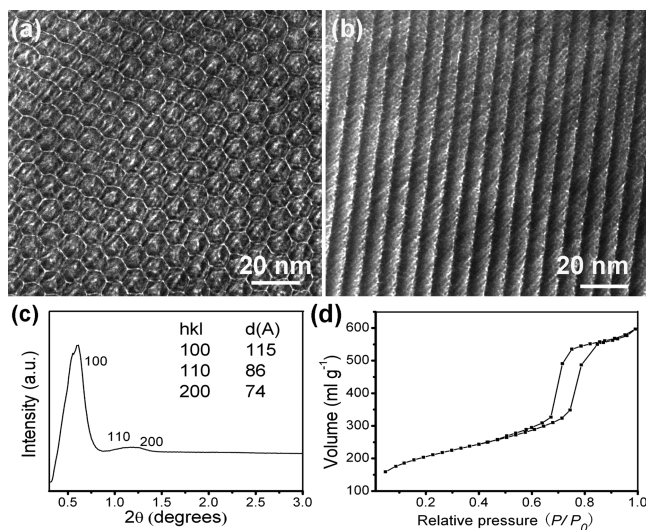


Figure 1. (a and b) HRTEM images showing top view and side view of the mesopores, respectively. (c) SAXS results. (d) N_2 adsorption–desorption isotherms which show a typical IV isotherm, with an N_2 hysteresis loop for the as-prepared HFMS sample.

aniline groups to form the second layer. On top of the second layer, two HFIP sensing groups are further grafted by reacting with two hexafluoroacetone trihydrate molecules. In addition, to avoid nonspecific environmental moisture adsorption on the hydrophilic mesoporous silica walls via the unreacted surface $\equiv\text{Si}-\text{OH}$ groups, hydrophobic molecules of chlorotrimethylsilane are modified to mask the unreacted $\equiv\text{Si}-\text{OH}$ groups [steps 3 and 4 in Scheme 1]. On the basis of TGA (thermogravimetry analysis; for a typical TGA curve, see Figure S2a in Supporting Information), the total amount of organic components grafted on the SBA-15 mesoporous silica is estimated to be about 13 wt %. The presence of HFIP groups in the as-prepared HFMS sample has been proved by FT-IR (see Figure S2b in Supporting Information). The strong peaks around 1215 cm^{-1} in the FT-IR spectrum are assigned to the C–F stretching. In the $^1\text{H}-^1\text{H}$ 2D NOESY spectrum (see Figure S3 in Supporting Information), the small peak at 7.9 ppm is attributed to the hydroxyl proton of the HFIP group, the peak at 5.1 ppm is assigned to the benzene ring, and the peak at 4.3 ppm is attributed to the amide. The $^1\text{H}-^1\text{H}$ 2D NOESY results further indicate that the hydroxyl proton of the HFIP group has a distinct correlation with the adjacent benzene ring. The HR-TEM images (see Figure 1a,b) show that the as-prepared HFMS sample preserved the high ordered hexagonal, $p6mm$, mesostructure of the mother SBA-15 mesoporous silica. This point is further proved by synchrotron SAXS (small-angle X-ray scattering) and N_2 gas adsorption (see Figure 1c,d). The results of SAXS and N_2 gas adsorption also indicate that the pore size obviously decreases from 7.5 nm of the mother SBA-15 to 5.8 nm of the as-prepared HFMS, while the wall thickness of HFMS increases from 3.4 to 7.4 nm, due to the introduced organic components (for a summary of data, see Table S1 in Supporting Information).

Application of HFMS for ppt Level TNT Vapor Detection. With an ultrasonic bath, the as-prepared HFMS is suspended in deionized (DI) water and then loaded onto the top surface of our developed resonant microcantilever¹⁷ using an Eppendorf micromanipulator. Figure 2a shows the HFMS-loaded cantilever, on which a resonance-exciting heater and a signal-readout

piezoresistor are integrated. The technical details of the cantilever are given in Experimental Section. Through an interface circuit, the sensing-layer loading-induced frequency-shift is shown in Figure 2b. On the basis of the 15 kHz frequency drop and the 1.53 Hz/pg mass sensitivity of the cantilever, about 10 ng of HFMS is loaded on the cantilever. According to the N_2 gas adsorption results, the HFMS used here is with a high specific surface area of $385 \text{ m}^2 \text{ g}^{-1}$. It can be estimated that about 4.3×10^{13} sensing terminals are modified on a $1 \times 10^4 \mu\text{m}^2$ area of the

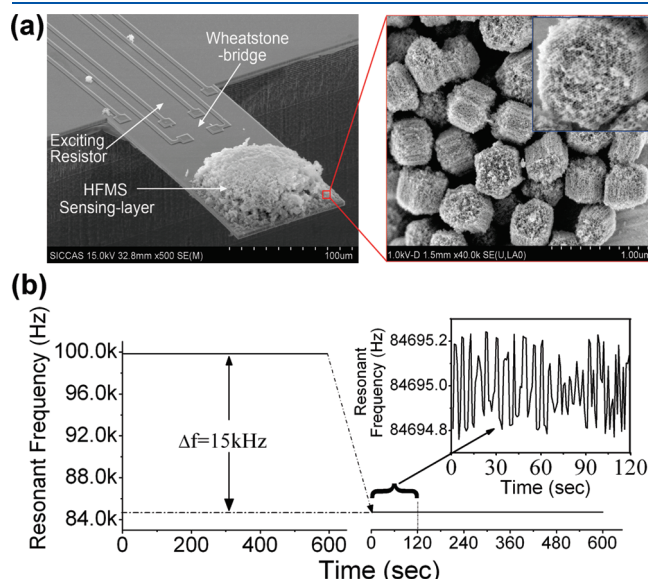


Figure 2. (a) FE-SEM image of the integrated silicon resonant microcantilever that is loaded with the HFIP-functionalized mesoporous silica sensing layer. (b) Tested 15 kHz frequency shift after loading the HFMS sensing layer, with an inset showing a frequency noise floor of about 0.4 Hz.

cantilever surface, according to the given molecular density ($5 \times 10^{18}/\text{m}^2$) on the SiO_2 surface.⁴⁹ Figure 2b also shows a low sensing signal noise floor of about 0.4 Hz.

The influence of SBA-15 physical characteristics, such as pore size and specific surface area, on sensing properties is considered. Obviously, the larger the pore size of SBA-15, the lower the specific surface area. The detailed data are listed in Table S1. In contrast, too small pore size (with high specific surface area) cannot accommodate TNT molecules. The mesoporous silica samples with pore size ranging from 4.8 to 13.8 nm are used as mother materials to prepare the HFMS for TNT-vapor sensing. The experimental results are illustrated in Figure 3a. The experiment verifies that an optimized pore size of the mesoporous silica can effectively enhance sensitivity, and herein a 7.5 nm pore size exhibits the highest sensitivity. With about a 1-nm-thick modification layer on the inner wall taken into account, the diameter of the functionalized pore will decrease from 7.5 to 5.8 nm. The experimental results indicate that the 5.8 nm pore size is just suitable for optimally adsorbing and desorbing TNT molecules (about 1 nm in diameter). Though a pore size larger than 5.8 nm is still usable for accommodating the TNT molecules, the larger pore size (see Table S1) would cause a smaller BET surface area, thereby suppressing the TNT-molecule adsorption efficiency. Figure 3b plots the sensing response of the HFMS-functionalized resonant cantilever to ultralow concentrations TNT vapor. When 45 ppt TNT vapor is introduced by injection into the testing chamber where the sensor is located, about 2.6 Hz frequency drop is observed that is about 6 times of the 0.4 Hz noise floor (see Figure 3b). When the concentration is increased to 90 ppt and 135 ppt, the corresponding output signal linearly increases (the response is approximately linear only for the ultralow concentration range). Figure 3c shows a repeated sensor response of 18 Hz to 380 ppt TNT vapor. The response time to TNT is about 1 min, the signal recovery time is about 2 min, and the interval for two consecutive detections is only

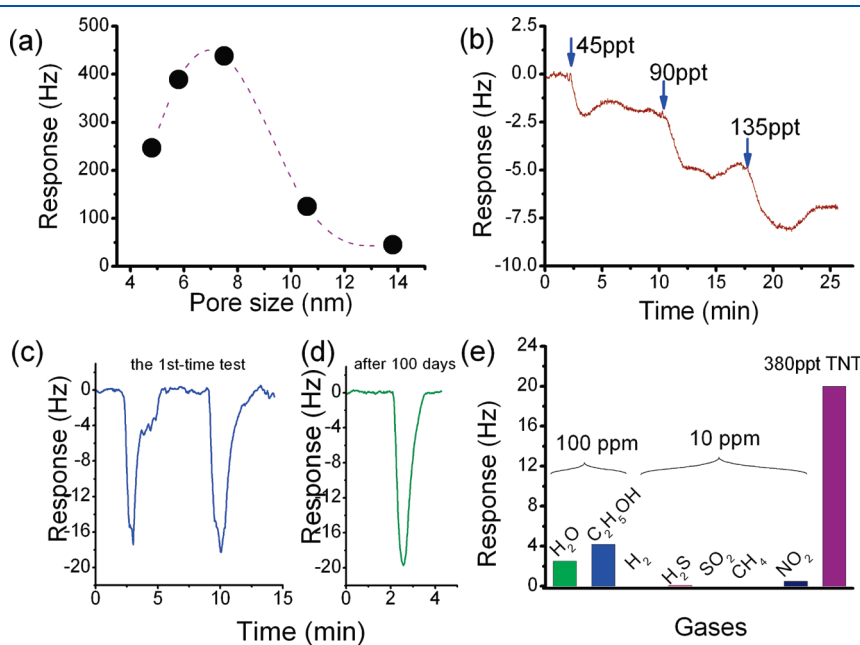


Figure 3. (a) Tested effect of pore size on TNT detection sensitivity. (b) Typical sensing responses of the functionalized HFMS sensor versus TNT at 45, 90, and 135 ppt. (c) Short-term repeatable and reversible rapid sensing response to 380 ppt TNT. (d) Subsequent detection with the same sensor after storage for 100 days, showing long-term stability of sensitivity. (e) Response of the TNT sensor to various kinds of interfering gases compared with response to 380 ppt TNT vapor.

7 min. To evaluate the long-term stability of the sensitivity, the same sensor is tested again after 100 days. The highly reproducible response shown in Figure 3d confirms the long-term reliability of the HFMS sensing material.

To compare the TNT sensing properties between the bare SBA-15 and the modified HFMS, a control experiment is conducted by using commercial QCM sensors (10 MHz). The sensing responses of the two materials (loaded on the QCMs, respectively) to 7.6 ppb TNT vapor are shown in Figure S4 of Supporting Information. The HFMS-loaded QCM possesses 4.4 times the sensitivity compared with that of the bare SBA-15-loaded QCM. Furthermore, the response speed of the bare SBA-15 to TNT is much lower than that of the HFMS because of the difference in specificity. Therefore, the HFIP-functionalization effect on the sensing properties is significant. On the other hand, the mother mesoporous silica has strong affinity to polar molecules (such as water). The high specific surface area can cause physical absorption. Furthermore, the large number of $\equiv\text{Si}-\text{OH}$ surface groups of the mother mesoporous silica can induce nonspecific absorption. Therefore, inner-wall modification to the mesoporous silica is necessary.

A selectivity experiment is also implemented, although the high specificity of the HFIP group to TNT molecules has been reported.⁸ In this experiment we select water (H_2O), ethanol ($\text{C}_2\text{H}_5\text{OH}$), hydrogen (H_2), hydrogen sulfide (H_2S), methane (CH_4), nitrogen dioxide (NO_2), and sulfur dioxide (SO_2) as interfering gases. Figure 3e shows that the TNT sensor exhibits lower than 5 Hz responses to all the interfering gases (100 ppm for water and ethanol, 10 ppm for the others). Because of the much higher sensor response to tens to hundreds of ppt TNT, satisfactory selectivity of the sensor has been achieved. Herein the high selectivity of the sensor in the presence of water is discussed. Pure mesoporous silica is a hydrophilic material, as there are a large number of silanol groups ($\equiv\text{Si}-\text{OH}$) on the pore surface that have strong affinity to water molecules. To solve the problem, we use self-assembled small hydrophobic organic molecules (chlorotrimethylsilane) to mask the surface-exposed unreacted $\equiv\text{Si}-\text{OH}$ groups during the functionalization process (see Scheme 1). In addition, we also use an ultrahydrophobic and oleophobic monolayer of FAS-17 to self-assemble on the SiO_2 surfaces of the resonant microcantilever to resist the nonspecific absorption of water and other small organic molecules.²⁰ According to our experimental results, the self-assembled FAS-17 effectively depresses the water interference signal by about 1 order of magnitude.

CMS Preparation, Characterization, and Application for Vapor Detection of Tens of ppb Ammonia and Its Derivatives. Functionalized with different groups, the mesoporous silica sensing material can be used to detect various VOC molecules. We also use COOH-functionalized mesoporous silica (CMS) to form ammonia (NH_3)/amine sensors. As a typical VOC vapor, NH_3 exists in livestock, indoor air, chemical plants, and elsewhere. As a derivative of NH_3 , trimethylamine (TMA) normally exists in fish muscle and can be detected to evaluate fish freshness. There have been many technologies to detect high concentrations of ammonia/amine^{50,51} and, practically, the human nose is sensitive to NH_3 in high concentration. However, it is hard to detect or smell ultralow concentrations of ammonia. For many purposes, there is a need to detect ammonia at the sub-ppm level. Metal oxide sensors are commercially available and widely used for ammonia detection. Unfortunately, such sensors have poor selectivity, and the detection limit is generally at the

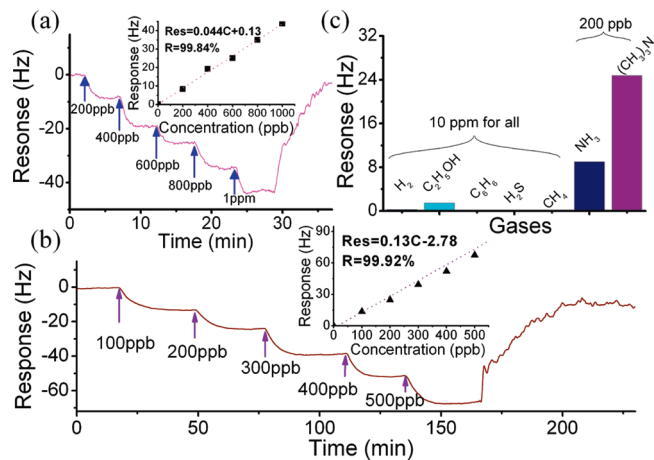


Figure 4. Typical response curves of the CMS sensor to NH_3 (a) and TMA (b) at various concentrations, where Res represents the response value and R represents the related coefficient. (c) Response of the cantilever CMS sensor to various kinds of interfering gases (all at 10 ppm concentration) compared with the response to 200 ppb NH_3 and 200 ppb TMA vapors.

level of tens of ppm. Although optical gas analyzers and chromatographers can detect a much lower concentration of ammonia, the high cost and large volume restrict them for portable use. Nessler's reagent can also be used for trace ammonia detection.⁵⁰ Unfortunately, the detection can only be conducted in water. By employing CuBr thin film as sensing material, another kind of resistive ammonia sensor has good sensitivity and selectivity to ammonia.^{52,53} However, its poor stability blocks the use of CuBr in ammonia detection because it is reactive to oxygen in the air.⁵³ Therefore, new amine-sensing materials should be developed.

It is known that there is a strong interaction between the COOH group and amines via base–acid reaction. On the other hand, the interference from other natural gases can be ignored, as there are few kinds of basic gas (except for ammonia/amines) existing in the environment. With the aforementioned situation considered, COOH-functionalized mesoporous silica (CMS) has the potential to be used in microgravimetric chemical sensors for trace amine detection. We use CES (carbomethoxysilanetriol, sodium salt, 25 wt % in water) as the key raw material to prepare CMS. FT-IR is used to prove the successful CMS preparation. The sharp peak at 1720 cm^{-1} is assigned to the vibration of the COOH group (see Figure S5a in Supporting Information). The TEM image (see Figure S5b in Supporting Information) shows that the as-prepared CMS still retains the mesoporous structure of its SBA-15 mother material. After CMS preparation, we use a method similar to that for the aforementioned TNT sensors to construct microcantilever ammonia/amine sensors.

Figure 4 shows two typical response outputs when the sensor is exposed to NH_3 and TMA, both at concentrations of hundreds of ppb. For NH_3 detection, increasing vapor concentrations in five steps (from 0 to 1 ppm, with an increment of 200 ppb for each step) are sequentially introduced to the sensor with 90 s for each step, and the corresponding sensor frequency signal linearly drops by about 7 Hz for every step. Finally, when the sensor is switched off from the 1 ppm gas, the recovery time of the sensor is shorter than 5 min.

The same cantilever sensor is then used to detect TMA. Various concentrations of TMA are introduced to the sensor

by repeated vapor injection (with a 100 ppb increment). Almost a linear frequency-shift response of the sensor is sequentially measured with a corresponding signal increment of about 13 Hz/100 ppb. However, it takes about 15 min to reach a saturated response for every testing step. After exposure to 500 ppb TMA, the sensor needs about 20 min to recover in clean air.

According to the results in Figure 4, the sensor shows a much higher response to TMA compared to NH₃. This may be explained as follows. If the functionalized CMS sensing material of the sensor adsorbs the same number of analyte molecules, TMA (molecule weight = 59) will generate a higher frequency drop than that of NH₃ (molecule weight = 17). Moreover, because the gas-phase basicity of TMA (948.9 kJ·mol⁻¹) is larger than that of NH₃ (819 kJ·mol⁻¹),⁵⁴ the COOH groups in the CMS sensing material adsorb more TMA molecules than NH₃. These two factors induce a higher response of the sensor to TMA than to NH₃. As a trade-off, both the response and recovery speeds of the sensor to TMA are slower than that to NH₃, as the bigger-sized TMA molecules are relatively difficult to move in the pore channel and the stronger gas-phase basicity of TMA causes more difficult desorption.

We also select H₂, NO₂, H₂S, C₂H₅OH, CH₄, and benzene (C₆H₆) as interfering gases to evaluate the selectivity of the ammonia/amine sensor. Figure 4c shows that the sensor always exhibits lower than 0.5 Hz response to all the interfering gases, which have identical concentrations of 10 ppm. Considering the specific reaction principle between the COOH-functionalized CMS sensing material and the basic gases, neither neutral gases (C₆H₆, H₂, C₂H₅OH, and CH₄) nor acidic gases (H₂S and NO₂) can cause significant sensor response. The negligible interference signal can only come from physical/nonspecific adsorption. Fortunately, except for the ammonia/amine vapors, other basic gases seldom exist in environmental air.

CONCLUSIONS

This study shows that functionalized mesoporous silica is a new kind of high-performance chemical sensing material for gravimetric sensors. Especially when the sensing materials are compatible with a miniaturized transducer platform such as the resonant microcantilever, detection of trace VOCs can be on-site, rapid, and portable. The satisfactory sensing results in this study indicate that functionalized mesoporous silica is promising in nose-on-a-chip applications.

ASSOCIATED CONTENT

Supporting Information. Additional information as described in the text. This material is available free of charge via the Internet at <http://pubs.acs.org>.

AUTHOR INFORMATION

Corresponding Author

*Tel: (+86) 21-62131794. Fax: (+86) 21-62131744. E-mail: xxli@mail.sim.ac.cn.

ACKNOWLEDGMENT

The research is supported by NSFC (60725414, 91023046), Chinese 973 Program (2011CB309503), and Korean WCU project (R32-2009-000-20087-0). The authors thank Prof. Jia-qiang Xu of Shanghai University, Dr. Yefeng Yao of East China

Normal University, and Dr. Zhijun Li and Dr. Yuzhu Wang of Shanghai Synchrotron Radiation Facility for helps with sample synthesis and characterization.

REFERENCES

- (1) Lindinger, W.; Hansel, A.; Jordan, A. *Chem. Soc. Rev.* **1998**, *27* (5), 347–354.
- (2) Lu, C. J.; Zellers, E. T. *Anal. Chem.* **2001**, *73* (14), 3449–3457.
- (3) Senesac, L.; Thundat, T. G. *Mater. Today* **2008**, *11* (3), 28–36.
- (4) Makinen, M. A.; Anttalainen, O. A.; Sillanpaa, M. *E. T. Anal. Chem.* **2010**, *82* (23), 9594–9600.
- (5) Yamazoe, N. *Sens. Actuators, B* **2005**, *108* (1–2), 2–14.
- (6) Lavrik, N.; Sepaniak, M.; Datskos, P. *Rev. Sci. Instrum.* **2004**, *75*, 2229–2253.
- (7) Mansfield, E.; Kar, A.; Quinn, T.; Hooker, S. *Anal. Chem.* **2010**, *82* (24), 9977–9982.
- (8) Grate, J. W. *Chem. Rev.* **2008**, *108* (2), 726–745.
- (9) Volk, S.; Schulein, F. J. R.; Knall, F.; Reuter, D.; Wieck, A. D.; Truong, T. A.; Kim, H.; Petroff, P. M.; Wixforth, A.; Krenner, H. J. *Nano Lett.* **2010**, *10* (9), 3399–3407.
- (10) Hartmann-Thompson, C.; Hu, J.; Kaganove, S. N.; Keinath, S. E.; Keeley, D. L.; Dvornic, P. R. *Chem. Mater.* **2004**, *16* (25), 5357–5364.
- (11) Goeders, K. M.; Colton, J. S.; Bottomley, L. A. *Chem. Rev.* **2008**, *108* (2), 522–542.
- (12) Yu, H. T.; Li, X. X. *Appl. Phys. Lett.* **2009**, *94* (1), 011901.
- (13) Liu, Y. J.; Li, X. X.; Zhang, Z. X.; Zuo, G. M.; Cheng, Z. X.; Yu, H. T. *Biomed. Microdevices* **2009**, *11* (1), 183–191.
- (14) Gupta, A.; Akin, D.; Bashir, R. *Appl. Phys. Lett.* **2004**, *84* (11), 1976–1978.
- (15) Campbell, G.; Mutharasan, R. *Anal. Chem.* **2006**, *78* (7), 2328–2334.
- (16) Betts, T. A.; Tipple, C. A.; Sepaniak, M. J.; Datskos, P. G. *Anal. Chim. Acta* **2000**, *422* (1), 89–99.
- (17) Yu, H. T.; Li, X. X.; Gan, X. H.; Liu, Y. J.; Liu, X.; Xu, P. C.; Li, J. G.; Liu, M. *J. Micromech. Microeng.* **2009**, *19* (4), 045023.
- (18) Xiang, Q.; Meng, G. F.; Zhang, Y.; Xu, J. Q.; Xu, P. C.; Pan, Q. Y.; Yu, W. J. *Sens. Actuators, B* **2010**, *143* (2), 635–640.
- (19) Xu, P. C.; Cheng, Z. X.; Pan, Q. Y.; Xu, J. Q.; Xiang, Q.; Yu, W. J.; Chu, Y. L. *Sens. Actuators, B* **2008**, *130* (2), 802–808.
- (20) Xu, P. C.; Li, X. X.; Yu, H. T.; Liu, M.; Li, J. G. *J. Micromech. Microeng.* **2010**, *20* (11), 115003.
- (21) Wan, Y.; Zhao, D. Y. *Chem. Rev.* **2007**, *107* (7), 2821–2860.
- (22) Johnson-White, B.; Zeinali, M.; Shaffer, K. M.; Patterson, C. H.; Charles, P. T.; Markowitz, M. A. *Biosens. Bioelectron.* **2007**, *22* (6), 1154–1162.
- (23) Tao, S. Y.; Li, G. T.; Zhu, H. S. *J. Mater. Chem.* **2006**, *16* (46), 4521–4528.
- (24) Ueno, Y.; Horiuchi, T.; Niwa, O.; Zhou, H. S.; Yamada, T.; Honma, I. *Sens. Actuators, B* **2003**, *95* (1–3), 282–286.
- (25) Zhang, H. X.; Cao, A. M.; Hu, J. S.; Wan, L. J.; Lee, S. T. *Anal. Chem.* **2006**, *78* (6), 1967–1971.
- (26) Trammell, S. A.; Zeinali, M.; Melde, B. J.; Charles, P. T.; Velez, F. L.; Dinderman, M. A.; Kusterbeck, A.; Markowitz, M. A. *Anal. Chem.* **2008**, *80* (12), 4627–4633.
- (27) Liu, Y.; Yu, Y. Y.; Yang, Q. Y.; Qu, Y. H.; Liu, Y. M.; Shi, G. Y.; Jin, L. T. *Sens. Actuators, B* **2008**, *131* (2), 432–438.
- (28) Fu, X. C.; Chen, X.; Wang, J.; Liu, J. H.; Huang, X. J. *Electrochim. Acta* **2010**, *56* (1), 102–107.
- (29) Keefe, M. H.; Slone, R. V.; Hupp, J. T.; Czaplewski, K. F.; Snurr, R. Q.; Stern, C. L. *Langmuir* **2000**, *16* (8), 3964–3970.
- (30) Allendorf, M. D.; Houk, R. J. T.; Andruszkiewicz, L.; Talin, A. A.; Pikarsky, J.; Choudhury, A.; Gall, K. A.; Hesketh, P. J. *J. Am. Chem. Soc.* **2008**, *130* (44), 14404–14405.
- (31) Ariga, K.; Ji, Q. M.; Hill, J. P.; Vinu, A. *Soft Matter* **2009**, *5* (19), 3562–3571.

- (32) Kresge, C.; Leonowicz, M.; Roth, W.; Vartuli, J.; Beck, J. *Nature* **1992**, *359* (6397), 710–712.
- (33) Hu, Y.; Bouamrani, A.; Tasciotti, E.; Li, L.; Liu, X. W.; Ferrari, M. *ACS Nano* **2010**, *4* (1), 439–451.
- (34) Fan, R.; Huh, S.; Yan, R.; Arnold, J.; Yang, P. D. *Nat. Mater.* **2008**, *7* (4), 303–307.
- (35) Torney, F.; Trewyn, B. G.; Lin, V. S. Y.; Wang, K. *Nat. Nanotechnol.* **2007**, *2* (5), 295–300.
- (36) Chen, Z.; Jiang, Y. B.; Dunphy, D. R.; Adams, D. P.; Hodges, C.; Liu, N. G.; Zhang, N.; Xomeritakis, G.; Jin, X. Z.; Aluru, N. R.; Gaik, S. J.; Hillhouse, H. W.; Brinker, C. J. *Nat. Mater.* **2010**, *9* (8), 667–675.
- (37) Joo, S. H.; Park, J. Y.; Tsung, C. K.; Yamada, Y.; Yang, P. D.; Somorjai, G. A. *Nat. Mater.* **2009**, *8* (2), 126–131.
- (38) Lu, Y. F.; Ganguli, R.; Drewien, C. A.; Anderson, M. T.; Brinker, C. J.; Gong, W. L.; Guo, Y. X.; Soyez, H.; Dunn, B.; Huang, M. H.; Zink, J. I. *Nature* **1997**, *389* (6649), 364–368.
- (39) Che, S.; Liu, Z.; Ohsuna, T.; Sakamoto, K.; Terasaki, O.; Tatsumi, T. *Nature* **2004**, *429* (6989), 281–284.
- (40) Han, Y.; Zhang, D. L.; Chng, L. L.; Sun, J. L.; Zhao, L.; Zou, X. D.; Ying, J. Y. *Nat. Chem.* **2009**, *1* (2), 123–127.
- (41) Madhugiri, S.; Dalton, A.; Gutierrez, J.; Ferraris, J. P.; Balkus, K. J. *J. Am. Chem. Soc.* **2003**, *125* (47), 14531–14538.
- (42) Coutinho, D.; Orozio-Tevan, R. A.; Reidy, R. F.; Balkus, K. J. *Microporous Mesoporous Mater.* **2002**, *54* (3), 229–248.
- (43) Zhao, D. Y.; Huo, Q. S.; Feng, J. L.; Chmelka, B. F.; Stucky, G. D. *J. Am. Chem. Soc.* **1998**, *120* (24), 6024–6036.
- (44) Zhao, D. Y.; Feng, J. L.; Huo, Q. S.; Melosh, N.; Fredrickson, G. H.; Chmelka, B. F.; Stucky, G. D. *Science* **1998**, *279* (5350), 548–552.
- (45) Zuo, G. M.; Li, X. X.; Zhang, Z. X.; Yang, T. T.; Wang, Y. L.; Cheng, Z. X.; Feng, S. L. *Nanotechnology* **2007**, *18* (25), 255501.
- (46) Grate, J. W.; Patrash, S. J.; Kaganove, S. N.; Wise, B. M. *Anal. Chem.* **1999**, *71* (5), 1033–1040.
- (47) Sepio, J.; Soulé, R. L. *J. Fluorine Chem.* **1984**, *24*, 61–74.
- (48) Li, L. P.; Liu, J. W.; Zhu, L. S.; Cutler, S.; Hasegawa, H.; Shan, B.; Medina, J. C. *Bioorg. Med. Chem. Lett.* **2006**, *16* (6), 1638–1642.
- (49) Feng, X.; Fryxell, G. E.; Wang, L. Q.; Kim, A. Y.; Liu, J.; Kemner, K. M. *Science* **1997**, *276* (5314), 923–926.
- (50) Timmer, B.; Olthuis, W.; van den Berg, A. *Sens. Actuators, B* **2005**, *107* (2), 666–677.
- (51) Yamamoto, M.; Kurihara, N.; Uchiyama, K.; Hobo, T. *Bunseki Kagaku* **2007**, *56* (7), 573–577.
- (52) Bendahan, M.; Jacolin, C.; Lauque, P.; Seguin, J. L.; Knauth, P. *J. Phys. Chem. B* **2001**, *105* (35), 8327–8333.
- (53) Zhang, Y. A.; Xu, P. C.; Xu, J. Q.; Li, H.; Ma, W. J. *J. Phys. Chem. C* **2011**, *115* (5), 2014–2019.
- (54) Bouchoux, G. *Mass Spectrom. Rev.* **2007**, *26* (6), 775–835.